JCB Article

AHNAK interaction with the annexin 2/S100A10 complex regulates cell membrane cytoarchitecture

Christelle Benaud,[1] Benoît J. Gentil,[1] Nicole Assard,[1] Magalie Court,[2] Jerome Garin,[2] Christian Delphin,[1] and Jacques Baudier[1]

[1]Laboratoire de Transduction du Signal, INSERM EMI-0104, DRDC-TS, and [2]Laboratoire de Chimie des Proteines, INSERM ERM-0201, DRDC-CP, CEA-Grenoble, 38054 Grenoble Cedex 9, France

Remodelling of the plasma membrane cytoarchitecture is crucial for the regulation of epithelial cell adhesion and permeability. In Madin-Darby canine kidney cells, the protein AHNAK relocates from the cytosol to the cytosolic surface of the plasma membrane during the formation of cell–cell contacts and the development of epithelial polarity. This targeting is reversible and regulated by Ca^{2+}-dependent cell–cell adhesion. At the plasma membrane, AHNAK associates as a multimeric complex with actin and the annexin 2/S100A10 complex. The S100A10 subunit serves to mediate the interaction between annexin 2 and the COOH-terminal regulatory domain of AHNAK. Down-regulation of both annexin 2 and S100A10 using an annexin 2–specific small interfering RNA inhibits the association of AHNAK with plasma membrane. In Madin-Darby canine kidney cells, down-regulation of AHNAK using AHNAK-specific small interfering RNA prevents cortical actin cytoskeleton reorganization required to support cell height. We propose that the interaction of AHNAK with the annexin 2/S100A10 regulates cortical actin cytoskeleton organization and cell membrane cytoarchitecture.

Introduction

AHNAK was first identified as a gene whose transcription is repressed in cell lines of neuroblastoma and some other tumors (Shtivelman et al., 1992). More recently, transcription of AHNAK was found to be subject to strong down-regulation by transforming Ras alleles in rodent fibroblasts (Zuber et al., 2000). AHNAK is a protein of an exceptionally large size (700 kD) that is encoded by an intronless gene located on human chromosome 11q12–13 (Shtivelman and Bishop, 1993; Kudoh et al., 1995). The deduced amino acid sequence of human AHNAK predicts a protein of 5,643 amino acids that can be divided into three main structural regions: the NH_2-terminal 251 amino acids, a large central region of 4,390 amino acids composed of the 128-aa unit repeated 26 times, and the COOH-terminal 1,002 amino acids. The recurrent 7-aa motif present within the AHNAK repeats, P-[ED]-[AVIL]-[ED]-L-[KR]-G, has striking similarities with repeated domains found in two other repeat-containing proteins, the giant sea urchin vesicle-associated protein (600 kD; Barton et al., 1992) and L-periaxin (147 kD; Dytrych et al., 1998). Several putative regulatory elements are clustered within the COOH terminus, including several NLSs (Nie et al., 2000), a leucine zipper (Shtivelman and Bishop, 1993), and several potential phosphorylation sites for PKB, PKC, and CKII (Sussman et al., 2001). The exact biological function of AHNAK is unknown, although several putative interacting proteins have been identified. In vitro, AHNAK fragments bind and activate PLCγ in the presence of arachidonic acid (Sekiya et al., 1999). AHNAK is also a major target protein for the calcium- and zinc-binding protein S100B (Gentil et al., 2001). In cardiomyocytes, AHNAK associates with the β subunit of cardiac L-type calcium channels at the plasma membrane, and is phosphorylated by PKA in response to adreno receptor stimulation (Haase et al., 1999). In vitro, the COOH-terminal AHNAK region (aa 5262–5643) binds to G-actin and cosediments with F-actin. A possible role for AHNAK in the maintenance of the structural and functional organization of the subsarcolemmal cytoarchitecture has been proposed (Hohaus et al., 2002). More recently, AHNAK immunoreactivity has been found within the lumen of specific vesicles called "enlargosomes," and is redistributed to the external surface of the plasma membrane in response to large increases in Ca^{2+}. Enlargosomes have been proposed to par-

The online version of this article includes supplemental material.

Address correspondence to Jacques Baudier, INSERM EMI-0104, DRDC-TS, CEA-Grenoble, 17 rue des Martyrs, 38054 Grenoble Cedex 9, France. Tel.: (33) 4-38-78-43 28. Fax: (33) 4-38-78-50-58. email: jbaudier@cea.fr

Key words: actin; calcium; cytoskeleton; cell adhesion; S100B

Abbreviation used in this paper: siRNA, small interfering RNA.

ticipate in cell membrane differentiation and repair (Borgonovo et al., 2002). A nuclear localization of AHNAK has also been reported (Shtivelman and Bishop, 1993; Sussman et al., 2001). During early mouse embryonic development, AHNAK is abundantly expressed in mesenchymal and epithelial cells at the major sites of morphogenesis, where it is essentially localized at the plasma membrane (Kingsley et al., 2001; Downs et al., 2002). In adult mice, AHNAK has a restricted tissue distribution. It is expressed at the plasmalemma of elastic tissues submitted to contracting and stretching forces and/or tissues forming in physical barriers that define body compartments. AHNAK is expressed in all muscular cells including cardiomyocytes, skeletal muscle cells, smooth muscle cells, fibromyocytes, and myoepithelial cells (Haase et al., 1999; Gentil et al., 2003). AHNAK is also highly expressed at the plasma membrane of lining epithelial cells (Hieda and Tsukita, 1989; Hashimoto et al., 1993; Gentil et al., 2003), but is absent from epithelia with secretory or absorptive functions (Gentil et al., 2003). The exact mechanisms by which AHNAK is localized to the plasma membranes remain to be investigated, especially because AHNAK does not possess a transmembrane domain. In the present work, we have developed cellular and molecular analyses to elucidate the function of AHNAK at the plasma membrane, and to identify proteins interacting with AHNAK in this cellular compartment. First, we show that at the plasma membrane, AHNAK interacts with the annexin 2/S100A10 complex, which regulates AHNAK plasma membrane localization. We also demonstrate that down-regulation of AHNAK affects the cell membrane cytoarchitecture of epithelial cells, and we propose a role of AHNAK in controlling the physical and mechanical properties of cell-peripheral membranes. Our results provide significant insights into the molecular mechanisms by which annexin 2 regulates cell membrane organization (Babiychuk et al., 2002; Gerke and Moss, 2002).

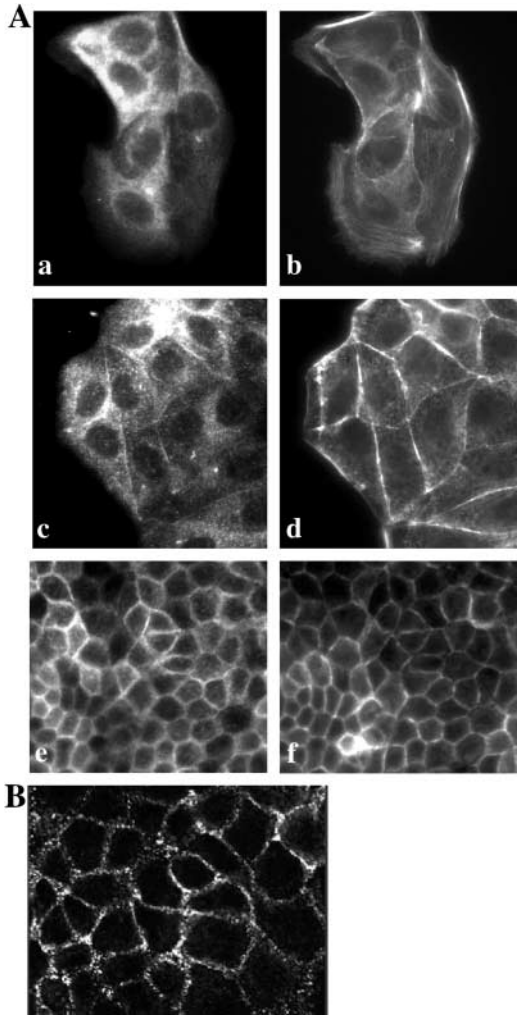

Figure 1. **Density-dependent localization of AHNAK to the cytoplasmic face of the MDCK cell plasma membrane.** (A) Redistribution of AHNAK and actin during confluence mediated cell–cell contact and polarization. MDCK cells were cultured on glass coverslips for 2 (a and b), 24 (c and d) or 96 h (e and f), and stained with anti-AHNAK-KIS antibody (a, c, and e) and F-actin visualized with phalloidin (b, d, and f). (B) Confocal immunofluorescence with polyclonal anti-AHNAK-KIS antibody of streptolysin O–permeabilized confluent MDCK cells reveals a positive signal at the cytoplasmic surface of the plasma membrane.

Results

AHNAK is redistributed at the cytosolic surface of the plasma membrane in confluent MDCK cells

In canine epithelial MDCK cells, AHNAK redistributes from the cytoplasm to a cortical/plasma membrane localization as cell density increases and as cells establish cell–cell contacts (Sussman et al., 2001; Fig. 1 A). This redistribution of AHNAK follows the reorganization of the actin cytoskeleton into cortical actin (Fig. 1 A). Three different AHNAK antibodies, the affinity-purified AHNAK-KIS pAb directed against the repeated central domain of AHNAK, the affinity-purified AHNAK-CQL pAb directed against the extreme COOH terminus (Gentil et al., 2003), and the anti-AHNAK (desmoyokin) antibody (DY) (Hashimoto et al., 1993) gave a similar immunostaining pattern. A recent work has shown that in secretory cell models, AHNAK can be localized within the lumen of specific vesicles called enlargosomes and is redistributed to the external surface of the plasma membrane in response to large increases in Ca^{2+} (Borgonovo et al., 2002). Therefore, we evaluated in confluent MDCK cells on which side of the plasma membrane AHNAK is distributed, and whether AHNAK is present in the lumen of cortical vesicles or in the cytoplasm. To resolve this issue, we compared the immunostaining obtained with our affinity-purified anti-AHNAK-KIS antibody in detergent-permeabilized cells, in streptolysin O–permeabilized cells, and in nonpermeabilized live confluent MDCK cells. In nonpermeabilized cells, no surface AHNAK immunolabeling was detected (unpublished data). When the plasma membrane of live cells was permeabilized with streptolysin O, a condition in which only cytoplasmic and not the vesicle luminal proteins are accessible to the antibodies, the plasma membrane was labeled (Fig. 1 B). An identical result was obtained with the anti-AHNAK (desmoyokin) antibody (DY) previously shown to recognize the membrane-bound protein in epithelial cells (Hashimoto et al., 1993, 1995; unpublished data). Even though we cannot exclude the possibility that a population of AHNAK is present in enlargosomes,

these results clearly indicate that in our epithelial cell model, AHNAK is predominantly a cytosolic protein localized at the intracellular face of plasma membrane.

Membrane-bound AHNAK interacts with the annexin 2/S100A10 complex

To gain further insight into AHNAK function at the plasma membrane, we sought to identify proteins interacting with AHNAK using coimmunoprecipitation coupled to mass spectrometry analysis. For convenient peptide sequence identification using human databases, we used human epithelial MCF-7 cells, which predominantly express AHNAK at the plasma membrane. Confluent MCF-7 cells were treated with the membrane-permeable cross-linker dithiobis succinimidyl propionate, and AHNAK was immunoprecipitated with anti-AHNAK-CQL antibodies. Proteins present within the AHNAK immunoprecipitate were reduced, separated by SDS-PAGE, and identified by mass spectrometry. One major protein recovered within AHNAK immunoprecipitate was identified as annexin 2 (Fig. S1, available at http://www.jcb.org/cgi/content/full/jcb.200307098/DC1). The interaction between AHNAK and annexin 2 was confirmed both by coimmunoprecipitation in absence of cross-linking with two independent antibodies directed against AHNAK and immunodetection, and by a pull-down approach using recombinant AHNAK fragments linked to the GST tag (Fig. 2 A). The COOH-terminal fragment of AHNAK (Cter; aa 4642–5643), but neither a central fragment of AHNAK (M1; aa 820–1330) nor the GST tag alone, interacted with annexin 2. The interaction of annexin 2 with AHNAK is specific because other annexin family members, annexin IV and annexin VI, are not recovered in the AHNAK immunoprecipitates or in the pull-down experiments.

At the plasma membrane, annexin 2 can form a tetrameric complex with the S100A10 subunit (Harder and Gerke, 1993), a protein that belongs to the S100 family of EF hand–type Ca^{2+}-binding proteins (Schafer and Heizmann, 1996). In contrast to other S100 proteins, S100A10 has lost the ability to bind Ca^{2+} (Gerke and Weber, 1985). Therefore, we examined whether S100A10 associates with annexin 2 when complexed to AHNAK. In both MCF-7 and MDCK cells, S100A10 is recovered together with annexin 2 in AHNAK immunoprecipitates (Fig. 2 B). The interaction of the annexin 2/S100A10 complex with AHNAK-Cter domain was confirmed in pull-down assays (Fig. 2 C). In MDCK cells metabolically labeled with [^{35}S]methionine/cysteine, two major proteins migrating with a molecular mass corresponding to annexin 2 and S100A10 bound specifically to the AHNAK-Cter domain (Fig. 2 C, left). The identity of these bands as annexin 2 and S100A10 was confirmed by Western blot analysis (Fig. 2 C, right). The interaction occurred in EDTA/EGTA-containing buffer, indicating that the interaction between AHNAK and annexin 2/S100A10 is Ca^{2+} independent.

To evaluate the contribution of S100A10 in the annexin 2/S100A10/AHNAK interaction, we examined the effect of the S100B protein on that interaction. Previously, we have shown that S100B, another member of the S100 family, interacts with AHNAK-Cter in a strict calcium-dependent manner (Gentil et al., 2001). Because striking structural similarities exist between S100A10 and Ca^{2+}-bound S100B (McClintock et al., 2002), we examined whether S100B can displace annexin 2/S100A10. First, we controlled that the interaction between the annexin 2/S100A10 complex and GST-AHNAK-Cter occurs in the presence of Ca^{2+}. Next, we observed that in the presence of Ca^{2+}, but not in EGTA (unpublished data), addition of recombinant S100B to the cell extracts fully antagonizes the binding of the annexin 2/S100A10 complex in a dose-dependent and competitive manner (Fig. 2 D). These data suggest that the annexin 2/S100A10- and S100B-binding domains on AHNAK-Cter overlap, and that S100A10 mediates the interaction between AHNAK and annexin 2.

The direct interaction of S100A10 with AHNAK was confirmed in vitro. When expressed in rabbit reticulocyte, S100A10 protein binds to and is pulled down by the recombinant GST-COOH-terminal domain of AHNAK (Fig. 2 E). No binding of rabbit reticulocyte that expressed annexin 2 could be detected (unpublished data). The direct interaction of S100A10 with AHNAK was also confirmed in yeast two-hybrid experiments. A human heart cDNA library was screened using the extreme COOH-terminal domain of AHNAK (CterC; aa 5124–5643) as a bait. 15 colonies were obtained out of 2×10^6 primary yeast transformants. The interaction specificity was retested after the mating assays on YC-UWLH medium and X-gal filter tests. Out of the 15 library plasmids retested, only two interacted specifically with CterC. The remaining plasmids gave a positive result with lamin and were considered as false positive. The nucleotide sequence of the two positive clones revealed that they correspond to S100A10. The specificity of interaction between S100A10 and CterC is illustrated in Fig. 2 F. Only CterC is competent for interaction with S100A10, and not CterN (aa 4642–5124), CterdLZ (aa 4642–4826), or lamin. Our double-hybrid experiment also reveals that S100B is capable of heterodimerizing with S100A10 in a yeast two-hybrid system (Fig. 2 F). Heterodimerization of S100B with other S100 proteins, such as S100A1, S100A6, and S100A11, has been observed previously (Deloulme et al., 2000). In contrast to the results obtained with S100A10, no interaction between S100B and AHNAK peptides could be detected in the yeast two-hybrid system (unpublished data). This is likely attributable to the limitation of yeast two-hybrid analysis to calcium-independent interactions (Deloulme et al., 2003).

AHNAK and the annexin 2/S100A10 complex are recruited to the sites of early cell–cell contacts

Confocal scanning immunofluorescence analyses of confluent epithelial MDCK cells reveal that AHNAK and annexin 2 colocalize all over the plasma membrane, including the sites of cell–cell contacts (Fig. 3 A). An identical pattern of distribution was observed for S100A10 (unpublished data). We had observed that AHNAK was recruited to the plasma membrane as cell confluence increased and as cells polarized (Fig. 1 A, e). The polarized phenotype of these cells was confirmed by the reorganization of the actin cytoskeleton (Fig. S2, available at http://www.jcb.org/cgi/content/full/jcb.200307098/DC1) and the apicolateral polarization of the tight junction marker ZO-1 (unpublished data). In po-

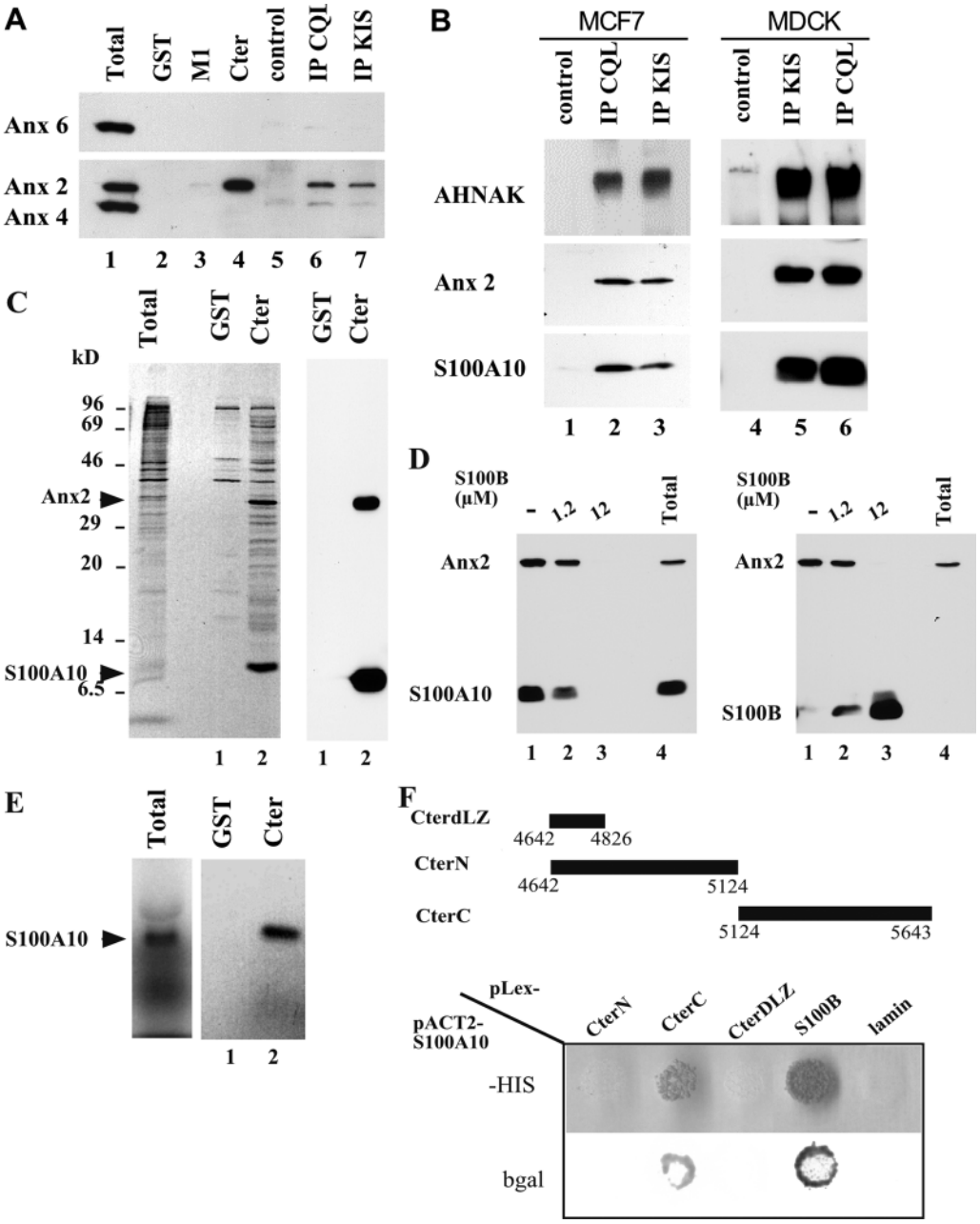

Figure 2. **Interaction of the annexin 2/S100A10 complex with AHNAK.** (A). MCF-7 cell extracts were incubated with glutathione-Sepharose (lanes 2–4) or protein A–Sepharose (lanes 5–7) in the presence of recombinant GST alone (lane 2), recombinant GST fused to AHNAK central repeat domain M1 (lane 3), recombinant GST fused to AHNAK COOH-terminal domain (lane 4), anti-AHNAK-CQL antibody (lane 6), or anti-AHNAK-KIS antibody (lane 7). Bound proteins were analyzed by Western blotting with anti-annexin 2, -4, and -6 antibodies. Lane 1 is total cell extract. (B). MCF-7 or MDCK cell extracts were incubated with control protein A-Sepharose beads (lanes 1and 4), or with anti-AHNAK-CQL (lanes 2 and 6) or anti-AHNAK-KIS (lanes 3 and 5) antibodies. Coimmunoprecipitated proteins were analyzed by Western blotting with anti-AHNAK-KIS, anti-annexin 2, and anti-S100A10 antibodies. (C) S100A10 and annexin 2 are the major proteins that interact with the AHNAK Cter domain. [^{35}S]Methionine/cysteine labeled MDCK whole-cell extracts (total; left) were incubated with GST (lane 1) and GST fusion AHNAK-Cter (lane 2) in EGTA/EDTA-containing buffer. Bound proteins were resolved on SDS-PAGE and were detected either by autoradiography (left) or blotted on nitrocellulose membrane and detected with mixed anti-annexin 2 and anti-S100A10 mAbs (right). (D) S100B antagonizes annexin 2/S100A10 binding to the AHNAK Cter domain. U87 cell extracts were incubated with GST fusion AHNAK-Cter in the absence (lane 1) or in the presence (lanes 2 and 3) of increasing S100B concentrations in Ca^{2+}/Zn^{2+}-containing buffer. Bound proteins were analyzed by Western blotting using anti-annexin 2 and anti-S100A10 antibodies (left), or with anti-annexin 2 and anti-S100B antibodies (right). Lane 4 is total cell extract. (E) [^{35}S]Methionine/cysteine-labeled S100A10 was produced in rabbit reticulocyte (total), and the translation reaction was incubated with glutathione-Sepharose in the presence of recombinant GST (lane 1) or recombinant GST fused to the AHNAK COOH-terminal domain (lane 2) in Ca^{2+}/Zn^{2+}-containing buffer. Bound proteins were resolved on SDS-PAGE and detected by autoradiography. (F) S100A10 specifically interacts with AHNAK CterC and S100B in the yeast two-hybrid system. Top: diagram of the various AHNAK COOH-terminal fragments used. Yeast were cotransfected with S100A10 pACT2 vector and different baits corresponding to AHNAK Cter deletion mutants, S100B, and lamin cloned into the pLEX vector as indicated. The interactions were scored by the growth of transfected yeast on YC-UWLH medium lacking histidine (HIS) and confirmed by β-galactosidase activity assay (bgal).

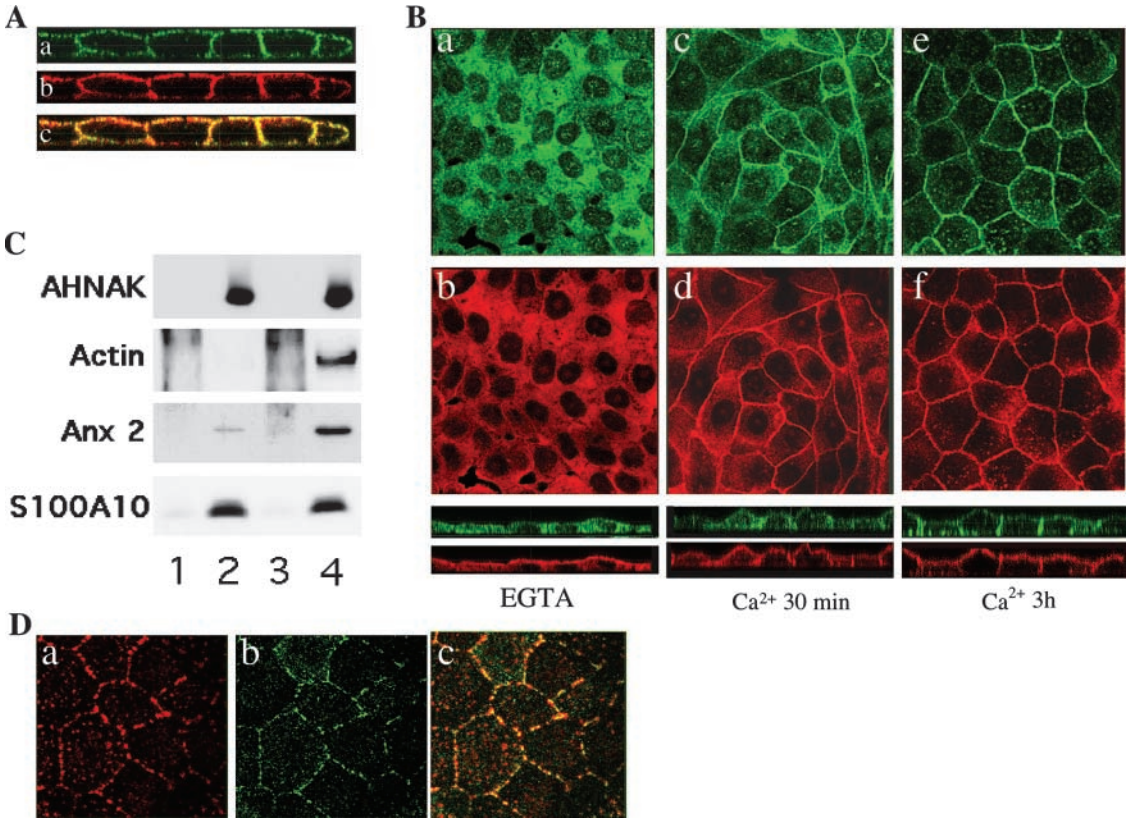

Figure 3. **AHNAK colocalizes with the annexin 2/S100A10 complex at the plasma membrane in MDCK cells.** (A) Confocal microscopy analysis (x-z axis) of the distribution in confluent MDCK cells of AHNAK (a), annexin 2 (b), and merge image (c). (B) Disruption of calcium-dependent cell–cell contacts causes the dissociation of AHNAK and annexin 2/S100A10 from the plasma membrane. Confluent MDCK cells were incubated in medium containing 5 mM EGTA supplemented with 1 mM $MgCl_2$ for 30 min at 37°C (a and b), and were then shifted to calcium-containing medium for 30 min (c and d) or 3 h (e and f). Cultures were double immunolabeled for AHNAK (a, c, and e) and S100A10 (b, d, and f). Single-plane confocal microscopy (x-y axis) and x-z section (bottom) images are shown. (C) Confluent MDCK cells incubated with EGTA-$MgCl_2$ medium for 30 min (lanes 1–2), then shifted back to Ca^{2+}-containing medium for 3 h (lanes 3 and 4), were cross-linked with dithiobis succinimidyl propionate. Whole-cell lysates were incubated with protein A–Sepharose beads (lanes 1 and 3) or anti-AHNAK-CQL antibody cross-linked onto Sepharose beads (lanes 2 and 4). Immunoprecipitated proteins were reduced and analyzed by Western blot with anti-AHNAK-CQL, anti-actin, mouse monoclonal anti-annexin 2, and anti-S100A10 antibodies. (D) Confocal immunofluorescence of actin stained with phalloidin (a) and AHNAK (b) in MDCK cells treated with 1 μg/ml cytochalasin D for 1 h (c) is the merged image.

larized epithelial cells, cell–cell contacts initiate plasma membrane remodelling and the development of cell polarity (Drubin and Nelson, 1996). Therefore, we tested the role of the formation of cell–cell contacts in recruiting AHNAK to the plasma membrane. Lowering the Ca^{2+} concentration in the culture medium of an MDCK monolayer interferes with the stability of intercellular contacts (Grindstaff et al., 1998). Treatment of confluent MDCK cells with low Ca^{2+} medium resulted in the redistribution of AHNAK and of the annexin 2/S100A10 complex from cell contacts to the cytoplasm, and correlated with a more flattened morphology of the cells (Fig. 3 B, a and b). This membrane dissociation of AHNAK and of the annexin 2/S100A10 complex was reversible (Fig. 3 B, c–f). When cell–cell contacts were allowed to reform by readdition of calcium into the culture medium, AHNAK and the annexin 2/S100A10 complex were recruited to the sites of cell–cell contacts with a similar kinetic of relocation and distribution pattern. Within 30 min of calcium addition, AHNAK and S100A10 started to relocate to the newly forming cell–cell contacts (Fig. 3 B, c and d), and to strongly accumulate there after 3 h, as cell acquired a more cuboidal epithelial morphology (Fig. 3 B, e and f). Coimmunoprecipitation experiments on cross-linked MDCK cells during the calcium switch experiment revealed that AHNAK forms a multimeric complex containing actin and annexin 2/S100A10, and that this association is strictly dependent on the localization of AHNAK at the plasma membrane (Fig. 3 C, lane 4). Upon membrane dissociation of AHNAK, only S100A10, and to a lesser extent annexin 2, are recovered within the AHNAK immunoprecipitates (lane 2).

The interaction of the membrane-bound form of AHNAK with the cortical actin cytoskeleton was confirmed by indirect immunofluorescence analysis of MDCK cells treated with cytochalasin D, which disrupts the integrity of the actin cytoskeleton (Fig. 3 D). As a consequence of its effect on actin, cytochalasin D treatment will also reversibly disrupt the organization of actin-associated membrane protein. In addition to the modification in the actin pattern, cytochalasin D treatment dramatically altered AHNAK distribution. At the apicolateral plasma membrane, AHNAK and actin precisely colocalized in a series of aggregates around the cell border, supporting the association of AHNAK with

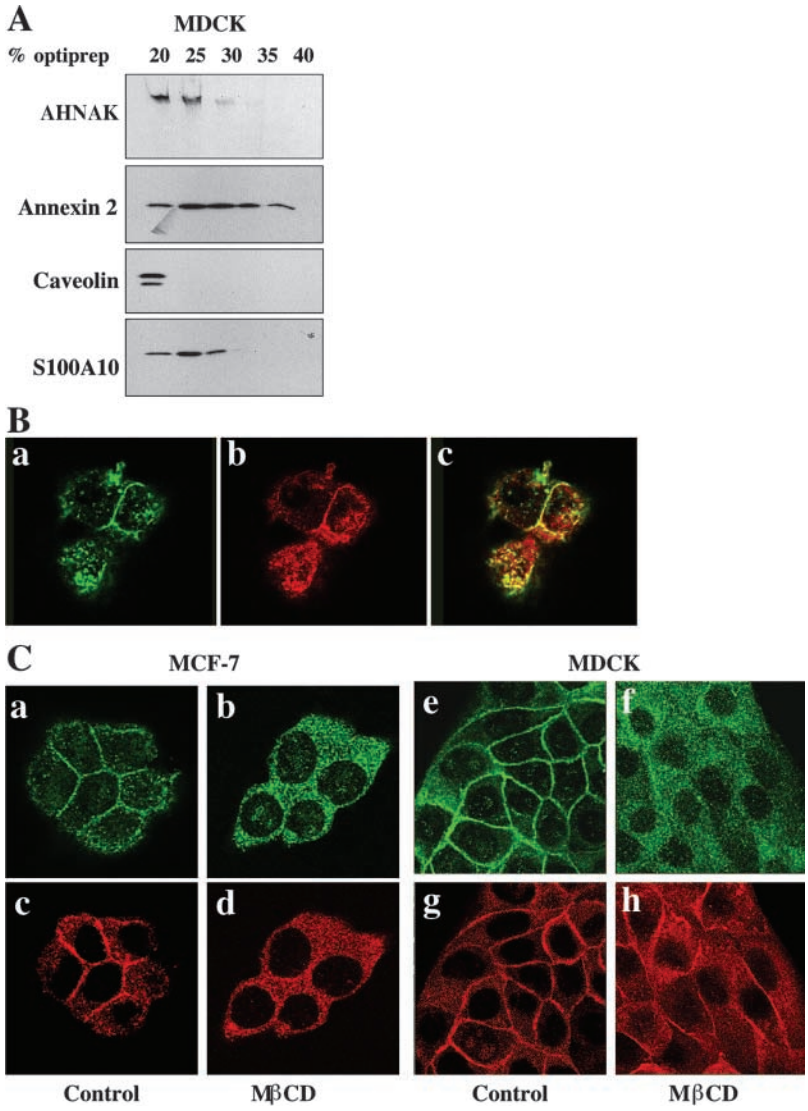

Figure 4. **AHNAK and annexin 2/S100A10 associate with cholesterol-rich membranes.** (A) AHNAK and annexin 2/S100A10 cofractionate to the lipid raft fractions. MDCK cells were lysed in buffer containing 1% Triton X-100 on ice, and flotation fractionation was performed in a 5–40% OptiPrep™ gradient. Fractions were analyzed by Western blotting using antibodies against AHNAK, annexin 2, and S100A10. Caveolin-1 was used as a marker of lipid raft–containing fraction. (B) Confocal microscopy analysis of FITC-cholera toxin β chain (a) and AHNAK (b) colocalization in MDCK cells. (c) Merged image. (C) Specific release of membrane-bound AHNAK by sequestration of membrane cholesterol. Confocal microscopy analysis of AHNAK (a, b, e, and f) and annexin 2 (HH7; c, d, g, and h) in MCF-7 (a–d) and MDCK (e–h) cells not treated (a, c, e, and g) or incubated with 3.8 mM of methyl-β-cyclodextrin (MβCD) for 15 min (b and d) or 1 h (f and h) at 37°C before fixation.

actin. Together, these data indicate that calcium-dependent cell–cell adhesion provides a signal for initiating the localized recruitment of AHNAK and annexin 2/S100A10 to sites of cell–cell contacts, where they form a stable protein complex with cortical actin cytoskeleton.

The annexin 2/S100A10/AHNAK complexes colocalize to intercellular junctions in a cholesterol-dependent mechanism

In addition to the Ca^{2+}-dependent association of annexin 2 with phospholipids, annexin 2 can also associate with the plasma membrane lipid raft microdomains in a cholesterol-dependent manner (Oliferenko et al., 1999; Babiychuk and Draeger, 2000; Babiychuk et al., 2002). Several laboratories have reported that annexin 2 may link lipid rafts with the cortical cytoskeleton (Oliferenko et al., 1999), and that annexin 2 recruits signaling proteins to intercellular junctions in a cholesterol-dependent manner (Hansen et al., 2002). To test a possible association of AHNAK with the annexin 2/S100A10 complex within lipid rafts, we performed flotation experiments in OptiPrep™ gradients in the presence of cold Triton X-100 (Fig. 4 A). In this gradient, the detergent-insoluble lipid rafts will float at the interphase between the 0 and 20% OptiPrep™ layers. In MDCK cells, a significant amount of AHNAK partitioned with annexin 2 and S100A10 into the lipid raft fraction together with caveolin-1, a known cholesterol-binding protein (Fig. 4 A). Not all the annexin 2 cosedimented with AHNAK, suggesting that only a portion of the annexin 2/S100A10 complex interacts with AHNAK and associates with the lipid rafts. We confirmed the association of AHNAK with lipid rafts in whole cells by colocalization of AHNAK with the FITC-labeled β subunit of cholera toxin, which specifically binds the lipid raft ganglioside GM1 (Harder et al., 1998). Confocal laser scanning microscopy of MCF-7 cells showed an extensive overlap of AHNAK staining with the FITC-labeled cholera toxin β chain at the plasma membrane, including intercellular junctions (Fig. 4 B). Furthermore, depletion of plasma membrane cholesterol in MDCK and MCF-7 cells with methyl-β-cyclodextrin released a population of annexin 2 from the plasma membrane and totally abolished the junctional membrane localization of AHNAK, causing their redistribution to the cell cytoplasm (Fig. 4 C).

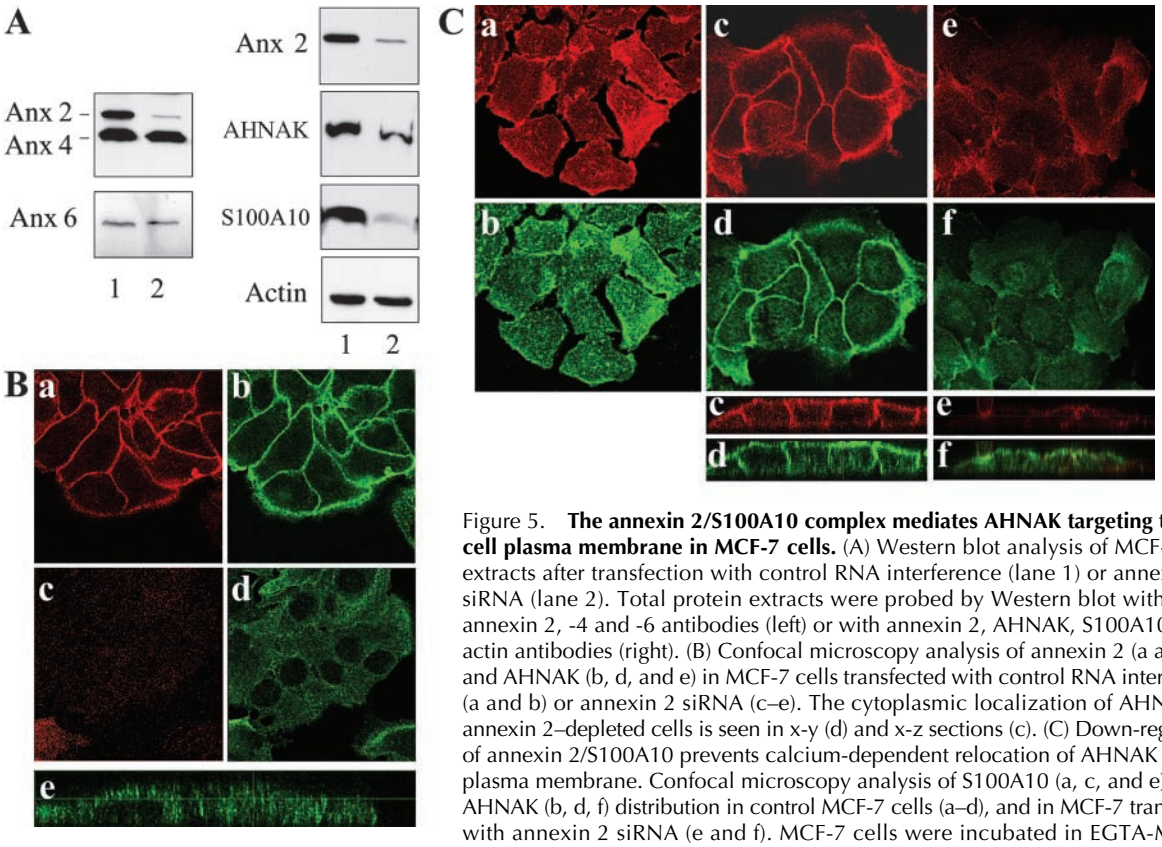

Figure 5. **The annexin 2/S100A10 complex mediates AHNAK targeting to the cell plasma membrane in MCF-7 cells.** (A) Western blot analysis of MCF-7 cell extracts after transfection with control RNA interference (lane 1) or annexin 2 siRNA (lane 2). Total protein extracts were probed by Western blot with anti-annexin 2, -4 and -6 antibodies (left) or with annexin 2, AHNAK, S100A10, and actin antibodies (right). (B) Confocal microscopy analysis of annexin 2 (a and c) and AHNAK (b, d, and e) in MCF-7 cells transfected with control RNA interference (a and b) or annexin 2 siRNA (c–e). The cytoplasmic localization of AHNAK in annexin 2–depleted cells is seen in x-y (d) and x-z sections (c). (C) Down-regulation of annexin 2/S100A10 prevents calcium-dependent relocation of AHNAK to the plasma membrane. Confocal microscopy analysis of S100A10 (a, c, and e) and AHNAK (b, d, f) distribution in control MCF-7 cells (a–d), and in MCF-7 transfected with annexin 2 siRNA (e and f). MCF-7 cells were incubated in EGTA-$MgCl_2$ medium for 30 min (a and b), then shifted to Ca^{2+}-containing medium for 3 h (c–f). Both x-y and x-z sections are shown.

Annexin 2/S100A10 down-regulation in MCF-7 cells interferes with membrane localization of AHNAK and cell height

To evaluate whether the annexin 2/S100A10 complex cooperates with AHNAK functions at the plasma membrane, we first analyzed the incidence of annexin 2 down-regulation on AHNAK subcellular localization. A small interfering RNA (siRNA) duplex was designed against the human annexin 2 cDNA sequence. This siRNA does not function in down-regulating canine annexin 2 in MDCK cells, but is highly efficient in human epithelial MCF-7 cells (Fig. 5 A). Transfection of MCF-7 cells with annexin 2 siRNA significantly abrogated the expression of annexin 2, but did not affect the levels of related annexins expressed in MCF-7, annexin 4, and annexin 6. The down-regulation of annexin 2 in MCF-7 cells induced a drastic concomitant down-regulation of S100A10. This was likely the result of both transcriptional and post-translational regulations of the S100A10 level by annexin 2, a previously described well-known phenomenon (Puisieux et al., 1996; Van de Graaf et al., 2003). A decrease in AHNAK levels was also observed in transfected cells. This effect of annexin 2 RNA interference on AHNAK levels was specific because the total level of actin was not affected, and the transfection with a nonspecific siRNA did not alter the levels of AHNAK (unpublished data). Consistent with the Western blot data, the membrane-associated AHNAK immunoreactivity dropped in annexin 2–depleted MCF-7 cells, and the remaining AHNAK signal appeared diffuse within the cytoplasm (Fig. 5 B). The interdependence that exists between the expression of annexin 2/S100A10 and the recruitment of AHNAK at the plasma membrane was confirmed in Ca^{2+} switch experiments (Fig. 5 C). As observed with MDCK cells (Fig. 3 B), disruption of calcium-dependent cell–cell contacts causes a reversible dissociation of AHNAK and of the annexin 2/S100A10 complex from the plasma membrane in MCF-7 cells (Fig. 5 C, a–d). However, in cells depleted with annexin 2/S100A10, AHNAK could not be re-recruited to the plasma membrane upon Ca^{2+}-mediated cell–cell adhesion, and cells retained a flattened morphology (Fig. 5 C, e and f).

Confocal microscopy analysis of actin distribution visualized with fluorescent phalloidin in control and annexin 2/S100A10-depleted cells confirmed the change in the morphology of cells with low annexin 2/S100A10 content (Fig. 6 A). The overall height of annexin 2/S100A10-depleted MCF-7 cells is decreased, with most of the actin-associated fluorescence found in the more basal focal planes. Similar changes in cell morphology and actin-associated fluorescence were also observed in MCF-7 cells depleted for AHNAK after transfection with AHNAK siRNA (Fig. 6 B; see following paragraph). Together, these data suggest that the membrane-associated annexin 2/S100A10 complex is essential to the recruitment of AHNAK at the plasma membrane, and that the annexin 2/S100A10/AHNAK complexes regulate actin-dependent cytoarchitecture.

AHNAK regulates the actin cytoskeleton scaffold of epithelial cells

To confirm the function of AHNAK in the regulation of cortical actin organization, we have down-regulated AH-

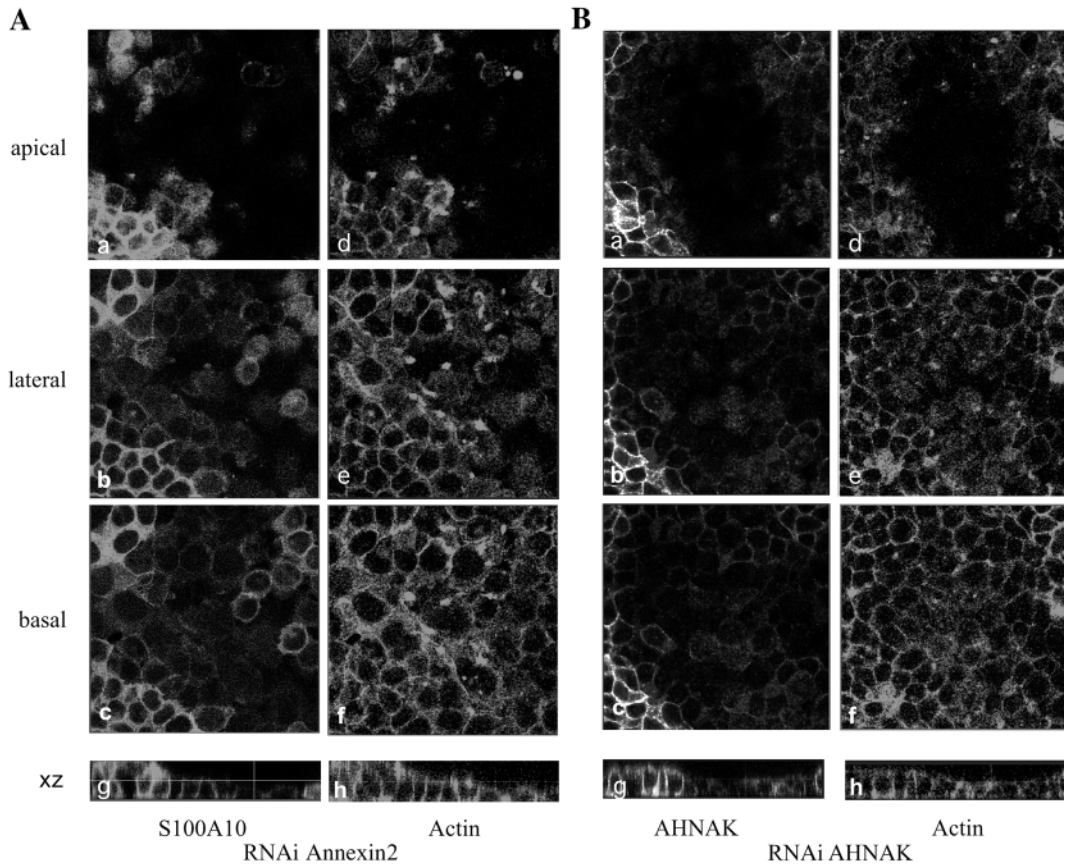

Figure 6. **Effect of the invalidation of AHNAK and annexin 2 on cell height.** Confocal images of MCF-7 cells transfected either with annexin 2 (A) or AHNAK (B) RNA interference. Apical (a and d), lateral (b and e), basal (c and f), and x-y sections and x-z merged sections (g and h) double immunostained for actin (A and B; d–f and h) and S100A10 (A; a–c and g) or AHNAK (B; a–c and g) reveals a similar collapse in cell height in both annexin 2– and AHNAK-invalidated cells. In A and B, x-y and x-z sections are from independent experiments.

NAK levels in MDCK cells, which rearrange their cytoskeleton in a highly structured manner as they polarize concomitantly with AHNAK recruitment to the plasma membrane (Fig. 1). An siRNA designed against the highly conserved repeated central domains of AHNAK efficiently and specifically down-regulates AHNAK levels in MDCK cells (Fig. 7 A; Fig. S3, available at http://www.jcb.org/cgi/content/full/jcb.200307098/DC1). We examined the effect of AHNAK siRNA on F-actin cytoskeleton rearrangement by confocal microscopy (Fig. 7, B–D). The extent of AHNAK down-regulation varied among transfected cells. Cells depleted for AHNAK were characterized by a marked disorganization of their actin cytoskeleton, visualized with fluorescent phalloidin. Unlike AHNAK-expressing cells, which rearranged their actin cytoskeleton into a lateral cortical belt and an apical actin network, cells devoid of AHNAK were unable to form an apicolateral cortical actin network, and F-actin could only be detected in the basal confocal plane (Fig. 7 B). AHNAK-negative cells retained a flattened morphology (Fig. 7 C). This decrease in cell height results in the void observed in the higher lateral and apical focal planes (Fig. 7 B, e and f). Note also that many AHNAK-negative cells at high density were dislodged from the cell monolayer and acquired rounded morphology (Fig. 7 B, arrows). This probably reflects an incapacity of invalidated cells to sustain density pressure because we did not observe a loss of adhesion of AHNAK-negative cells at low density (unpublished data). Although down-regulation of AHNAK has a drastic effect on actin cytoskeleton organization at the apicolateral plasma membrane that acts to support cell height, it has only a subtle effect on the basal actin organization. Cells invalidated for AHNAK only displayed more punctuate actin stress fibers on their basal side, compared with control cells (Fig. 7 D). Note also that in AHNAK-depleted cells, the annexin 2/S100A10 complex remains localized at the plasma membrane (unpublished data). This observation indicates that annexin 2/S100A10 is not sufficient to regulate actin cytoskeleton organization that acts to support cell height, and argues for a direct cooperation with AHNAK. Together, our data suggest that AHNAK regulates cortical actin cytoskeleton organization.

Discussion

In epithelial cells, AHNAK is predominantly a cytosolic protein localized at the plasma membrane intracellular face. A faint AHNAK immunoreactivity within the cell nuclei was observed in cells submitted to a Ca^{2+} switch (Fig. 5 C), but was never observed in other cell culture conditions. The apparent exclusive cytoplasmic localization of AHNAK in MDCK cells contrasts with the results of Shtivelman's group, who reported nuclear localization of AHNAK in

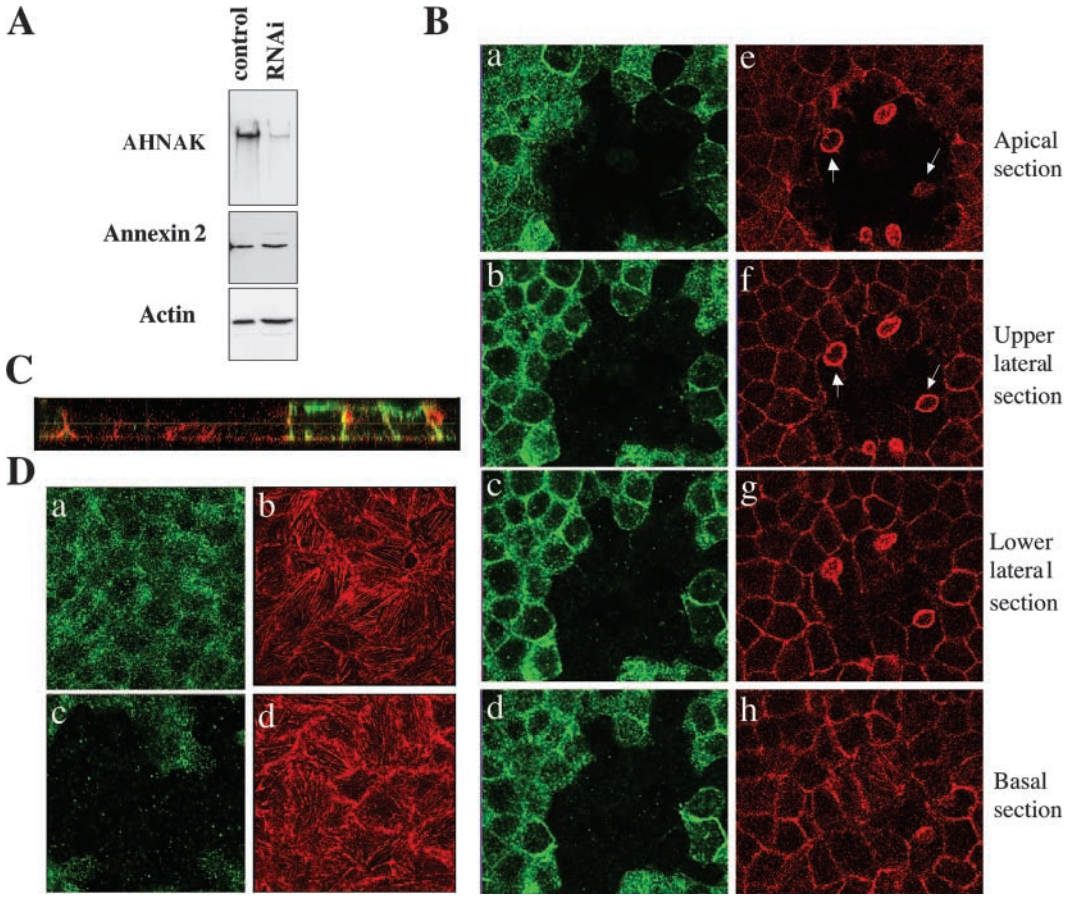

Figure 7. **AHNAK regulates actin-based cell membrane cytoarchitecture.** (A) Down-regulation of AHNAK by siRNA in MDCK cells. Total cell lysates of cells treated with AHNAK RNA interference or control RNA interference were analyzed by Western blot for AHNAK, annexin 2, and actin levels. (B) Effect of AHNAK siRNA on actin organization. MDCK cells transfected with AHNAK RNA interference were stained for AHNAK (a–d) and F-actin (e–h) with phalloidin. Confocal x-y sections at the apical (a and e), upper lateral (b and f), lower lateral (c and g), and basal (d and h) levels of the cells show that cells devoid of AHNAK are unable to form an apicolateral cortical actin network, leaving a black void in the higher apicolateral planes. Rounded AHNAK-negative cells can be seen within the monolayer (arrows). (C) Confocal microscopy x-z merged sections of AHNAK (green) and actin (red) staining reveals that cells invalidated for AHNAK retains a flattened morphology. (D) The effect of AHNAK siRNA on basal actin stress fibers. Basal confocal microscopy section shows that cells invalidated for AHNAK (c and d) displayed disorganized actin stress fibers on their basal side, compared with control cells (a and b).

sparse MDCK cell cultures (Sussman et al., 2001). Several possible explanations could be envisioned to explain the apparent discrepancies in subcellular AHNAK localization in MDCK cells. Some discrepancies can arise from the well-known heterogeneities in specific cell lines or clones in the various laboratories. Differences in epitope accessibility might also have to be considered. AHNAK nuclear immunoreactivity has only been reported with one antibody, FEN (Shtivelman and Bishop, 1993; Sussman et al., 2001). Because a recent work has pointed out that FEN cross reacts with a nuclear protein that is not recognized by two other AHNAK-specific antibodies (Borgonovo et al., 2002), we suggest that when located within the cell nuclei, AHNAK may adopt a conformation that could only be revealed by a specific antibody such as FEN.

In cultured epithelial cells, AHNAK targeting to the plasma membrane is reversible and triggered by Ca^{2+}-dependent cell adhesion. Disruption of E-cadherin–mediated cell–cell contacts by low extracellular Ca^{2+} results in the dissociation of AHNAK from the plasma membrane. After readdition of Ca^{2+}, AHNAK is rapidly re-recruited to the plasma membrane at the sites of newly formed cell–cell contacts. In contrast to the tight junction-associated protein ZO-1, AHNAK immunoreactivity will progressively become more widely distributed all over the plasma membrane (unpublished data). In fully polarized MDCK cells, AHNAK immunoreactivity decorates the entire basal, lateral, and apical cell membranes. Such distribution of AHNAK suggests that AHNAK is not a junctional protein. Down-regulation of AHNAK levels in MDCK cells using AHNAK-specific siRNA prevents cortical actin cytoskeleton reorganization. These observations suggest a more general function for AHNAK in organizing cell cytoarchitecture at the plasma membrane.

To gain further insight into the molecular mechanisms of AHNAK function at the plasma membrane, we have searched for AHNAK partners at the plasma membrane. We have identified the annexin 2/S100A10 complex as a major AHNAK-binding protein in epithelial cells. Annexin 2 (also called calpactin I heavy chain, p36) is a member of the annexin family of Ca^{2+}- and phospholipid-binding proteins, which has been implicated in membrane trafficking and organization (for review see Gerke and Moss, 2002). Annexin

2 has been proposed to play a role in the organization of cholesterol-rich membrane microdomains (Oliferenko et al., 1999), the connection of lipid rafts with the under lying actin cytoskeleton (Harder et al., 1997; Gerke and Moss, 2002), and in cholesterol-mediated adherent junction formations (Harder et al., 1997; Corvera et al., 2000). Within cells, annexin 2 can occur either as a monomer or as a heteroterameric complex coupled with S100A10 (also called calpactin I light chain, p11). The heterotetrameric annexin 2/S100A10 complex is the predominant form of annexin 2 present at the plasma membrane in epithelial cells (Harder and Gerke, 1993). The interaction between AHNAK and annexin 2/S100A10 occurs within the COOH-terminal domain of AHNAK. The direct interaction of S100A10 with the extreme COOH-terminal domain of AHNAK observed in vitro and in yeast two-hybrid experiments strongly suggests that S100A10 mediates the interaction between AHNAK and annexin 2. The physical interaction between AHNAK and the annexin 2/S100A10 complex in the cell is supported by several observations. First, a strict correlation exists between accumulation of AHNAK and the annexin 2/S100A10 complex to the plasma membrane during both confluence-mediated (Hansen et al., 2002; Fig. 1 A) and Ca^{2+}-dependent cell–cell adhesion (Fig. 3). Second, at the plasma membrane, AHNAK colocalizes with the annexin/S100A10 complex, and a significant amount of proteins associate with membrane rafts in a cholesterol-dependent manner (Fig. 4). Third, annexin 2 depletion by siRNA promotes AHNAK release to the cytoplasm (Fig. 5, B and C). The annexin/S100A10 dependence for AHNAK membrane localization strongly suggests that annexin 2/S100A10 contributes to the recruitment and stabilization of AHNAK at the plasma membrane. Two recent reports have pointed out a role for S100A10 in targeting channel proteins to the plasma membrane (Girard et al., 2002; Van de Graaf et al., 2003). A more general function for the annexin 2/S100A10 in the routing of proteins to the plasma membrane must now be considered.

Membrane-bound AHNAK not only interacts with annexin 2/S100A10, but also is part of a complex containing actin (Fig. 3, C and D). This observation is consistent with a recent paper describing physical interaction between AHNAK and F-actin and G-actin (Hohaus et al., 2002), and strongly suggests that AHNAK and annexin 2/S100A10 are part of a submembranous complex that interacts physically with the cortical actin cytoskeleton. Annexin 2/S100A10- and AHNAK-depleted MCF-7 cells both display decreased cell height. A similar and more drastic effect is observed in polarized epithelial MDCK cells, which retain a mesenchymal morphology upon AHNAK depletion (Fig. 7). Downregulation of AHNAK prevents the apicolateral actin cytoskeleton reorganization required to support cell height. We propose that AHNAK and the annexin 2/S100A10 complex are involved in the regulation of the actin cytoskeleton organization at the lateral plasma membrane, and thus could be implicated in plasma membrane remodelling and in the establishment of specialized intercellular interaction. Such a role for AHNAK is consistent with its specific expression in most lining epithelium and in endothelial cells of impermeable brain capillaries and peripheral blood vessels, and conversely with its absence in the highly permeable fenestrated endothelium of the kidney glomeruli, the hepatic sinusoid, and the continuous capillaries of lung (Gentil et al., 2003). In adult tissues, AHNAK is also abundantly expressed at the plasma membrane of smooth muscle cells (Gentil et al., 2003). In smooth muscle cells, annexin 2 is thought to function as a cross-linker of lipid rafts with the underlying actin cytoskeleton to regulate sarcolemmal tension (Babiychuk and Draeger, 2000; Babiychuk et al., 2002). In these cells, AHNAK may cooperate with annexin 2 in the coordination of cytoskeletal and membrane rearrangements—a coordination that provides structural support of the membrane to respond to and control stretching forces (Babiychuk and Draeger, 2000; Babiychuk et al., 2002). A similar role for AHNAK has already been suggested in cardiac muscle (Hohaus et al., 2002). Although our paper highlights a structural role of AHNAK, the association of AHNAK with lipid rafts also opens the possibility that AHNAK could be implicated in regulation of signaling pathways that are compartmentalized within these microdomains (Simons and Toomre, 2000; Zajchowski and Robbins, 2002).

Materials and methods

Cell culture

U87 glioblastomes, MCF-7, and MDCK epithelial cells were maintained in DME (Life Technology), 10% FBS (Sigma-Aldrich), and 1% penicillin/streptomycin.

For calcium switch experiments, cells were incubated for 30 min with DME supplemented with 5 mM EGTA and 1 mM $MgCl_2$ to lower extracellular Ca^{2+} concentration and to perturb strict Ca^{2+}-dependent cell–cell adhesion, but to maintain Mg^{2+}-dependent cell–matrix adhesion. Cell–cell contacts were allowed to reform for the indicated times by returning cells to complete medium.

Reagents and antibodies

The pAbs directed against AHNAK, KIS, and CQL have been described previously (Gentil et al., 2003). Anti-annexin 2 mAb HH7 was a gift from V. Gerke (Universiy of Münster, Münster, Germany). Anti-annexin 2, anti-annexin 2 light chain (S100A10), anti-annexin IV, anti-annexin VI, and anti-caveolin-1 mAbs were purchased from Transduction Laboratories. Texas red–phalloidin was purchased from Molecular Probes, Inc., and anti-actin mAb was purchased from Sigma-Aldrich. FITC-labeled cholera toxin B subunit and the cholesterol chelator methyl-β-cyclodextrin were purchased from Sigma-Aldrich.

In vitro protein–protein interaction assay/GST pull-down

GST-AHNAK-Cter and GST-AHNAK-M1 proteins (Gentil et al., 2001) were produced in the *Escherichia coli* AD494(DE3)pLYsS strain (Novagen) and purified by glutathione-Sepharose affinity chromatography. For metabolic labeling, cells were labeled in methionine-free MEM and 5% FCS supplemented with 50 μCi/ml [^{35}S]methionine/cysteine mix for 12 h. For binding assays, cells were lysed at 4°C in TTBS buffer (40 mM Tris-HCl, pH 7.5, 150 mM NaCl, and 0.3% Triton X-100) plus protease inhibitors (leupeptin, aprotinin, pepstatin, and AEBSF; 10 μg/ml each), and were centrifuged for 10 min. Cell lysates were precleared by incubation for 10 min with 50 μl GST-Sepharose. 500-μl aliquots of precleared supernatant were supplemented with either 5 mM EDTA/5 mM EGTA or with 0.3 mM $CaCl_2$/10 μM $ZnSO_4$ and mixed with 10 μg purified GST fusion proteins plus 30 μl affinity GST-Sepharose beads equilibrated in the same buffers. After mixing for 15 min at 4°C, the beads were spun down and the supernatant was removed. The beads were washed three times with 1 ml binding buffers. At the last wash, beads were transferred to new tubes and boiled in SDS sample buffer.

Mass spectrometric analysis and protein identification

Proteins recovered within AHNAK immunoprecipitates were excised from Coomassie blue–stained gels and washed with 50% acetonitrile. Gel pieces were dried in a vacuum centrifuge and rehydrated in 20 μl of 25

mM NH_4HCO_3 containing 0.5 μg trypsin (sequencing grade; Promega). After 4 h incubation at 37°C, a 0.5-μl aliquot was removed for MALDI-TOF analysis and spotted onto the MALDI sample probe on top of a dried 0.5-μl mixture of 4:3 saturated α-cyano-4-hydroxy-trans-cinnamic acid in acetone/10 mg/ml nitrocellulose in acetone/isopropanol 1:1. Samples were rinsed by placing a 5-μl volume of 0.1% TFA on the matrix surface after the analyte solution had dried completely. After 2 min, the liquid was blown off by pressurized air. MALDI mass spectra of peptide mixtures were obtained using a mass spectrometer (Bruker Biflex; Bruker-Franzen Analityk). Internal calibration was applied to each spectrum using trypsin autodigestion peptides (MH+ 842.50, MH+ 1045.55, and MH+ 2211.11). Protein identification was confirmed by tandem mass spectrometry experiments as described previously (Gentil et al., 2001).

Double hybrid

For plasmid constructions, fusion proteins with LexA DNA-binding domain (LexADBD) were constructed in pLex10. For the pLex-AHNAK Cter construction, BamHI–EcoRI AHNAK fragment (aa 4642–5643) from pDY-C (Nishimoto) was subcloned into pcDNA3.1. The insert was then excised with BamHI and XhoI digestion and cloned into BamHI–SalI sites of pLex10. pLex-CterN was obtained by deleting AHNAK pstI–pstI fragment from pLex-AHNAK Cter. To obtain the pLex-AHNAK-CterC construct, pstI–pstI AHNAK fragment (aa 5124–5643) of pLex-AHNAK Cter was subcloned into the pstI site of plex10. For the pLex-Cter-LZ construct, the pLex-CterN plasmid was deleted by SalI–PstI digestion, blunted with Deep vent polymerase, and self ligated. pLexS100B was obtained by amplification of human S100B cDNA using primers containing SmaI and pstI sites immediately flanking the start and the stop codon, respectively, and cloning of the PCR product into SmaI–pstI sites of pLex10.

Large-scale yeast transformations using the human heart Matchmaker™ cDNA library constructed in pACT2T plasmid (CLONTECH Laboratories, Inc.) and two-hybrid screens were performed using an L40 yeast strain essentially as described previously (Deloulme et al., 2000). Primary transformants were analyzed on YC-UWLH medium plates. Growing clones were then tested for β-galactosidase expression (Deloulme et al., 2000). Library plasmids expressing LEU2 from positive transformants were selected using HB101 *E. coli*, which requires leucine supplementation for growth. cDNAs were retested in a mating assay against the original bait construct and pLexA-lamin as a control using the AMR70 yeast strain as described below. The interactions were also tested by yeast mating essentially as described previously (Deloulme et al., 2000).

Immunoprecipitation and Western blotting

For total cell lysates and coimmunoprecipitation, cells were washed in PBS and lysed on ice in lysis buffer (50 mM Tris, pH 8.0, 150 mM NaCl, 0.05% deoxycholic acid, 1% Triton X-100, 10% glycerol, 2 mM EDTA/EGTA, and protease inhibitor cocktail). Lysates were passed through a 26G needle and centrifuged for 10 min at 2,500 rpm in a tabletop centrifuge. Supernatants were either quantified with the BCA protein micro assay (Pierce Chemical Co.) and boiled in 1× DTT Laemmli buffer (total cell lysates), or incubated with either anti-AHNAK-KIS antibody together with protein A–Sepharose (Amersham Biosciences), anti-AHNAK-CQL antibody cross-linked onto Sepharose beads, or with protein A–Sepharose alone, for 1 h rotating at 4°C. The immunoprecipitates were washed three times in lysis buffer, and the beads boiled in 1× Laemmli with 20 mM DTT. Proteins were separated by SDS-PAGE using 5, 8, or 14% polyacrylamide concentrations to resolve AHNAK, actin, or annexin 2/S100A10, respectively. Proteins were blotted onto nitrocellulose membranes.

For cross-linking experiments, cells were washed in PBS, incubated for 5 min with 0.5 mM dithiobis succinimidyl propionate (Pierce Chemical Co.) in PBS, and washed twice in 50 mM glycine in PBS before cell lysis and AHNAK immunoprecipitation. Immunoprecipitated proteins were reduced by boiling for 5 min in 1× Laemmli buffer containing 5% β-mercaptoethanol, and were analyzed by Western blot.

RNA interference

21-nt siRNA duplexes targeting the 5′-AAGAUCUCCAUGCCUGAUGUG-3′ mRNA sequence in the repeated domains of *ahnak*, and the 5′-AAGUGCAUAUGGGUCUGUCAA-3′ mRNA sequence corresponding to the NH_2-terminal domain of human *annexin 2* were purchased from Dharmacon. The sequence used was submitted to a BLAST search to ensure targeting specificity. The specificity of AHNAK and annexin 2 down-regulation was further checked by Western blotting analysis. MCF-7 or MDCK cells plated at low density ($3 \times 10^4/cm^2$) were transfected with 20 nM of either annexin 2 or AHNAK siRNA duplex, or scrambled siRNA using Oligofectamine™ (Life Technologies) on two consecutive days, and maintained for a total of 4 d in DME 10% serum.

Immunofluorescence

Cells were either fixed in 4% PFA for 10 min at RT, followed by a permeabilization with 0.1% Triton X-100 for 10 min or with 70% methanol at −20°C for 10 min. Cells were then washed in TBS and incubated with the primary antibody in TBS containing 3% goat serum overnight at 4°C. After TBS washes, cells were then incubated for 1 h at RT with the secondary antibody in TBS goat serum, and phalloidin when required. The secondary antibodies coupled with Alexa® 488 were purchased from Molecular Probes, Inc., and those coupled with Cy3 and Cy5 were purchased from Jackson ImmunoResearch Laboratories. After the final washes, cells were mounted in fluorescence mounting medium (DakoCytomation) and analyzed with a fluorescent microscope (Axiovert 200M; Carl Zeiss MicroImaging, Inc.) or a confocal microscope (TCS-SP2; Leica).

For plasma membrane permeabilization, cells were treated with 0.5 U streptolysin O (Sigma-Aldrich) in 0.1% BSA-PBS at 4°C and transferred at 37°C for 5 min. Cells were then washed with PBS and incubated with the primary antibody diluted in PBS/5% goat serum for 30 min at 4°C. After PBS washes, cells were fixed with 4% PFA and processed as above.

Cholera toxin labeling of GM1

MCF-7 cells were incubated with 0.5 μg/ml FITC-labeled cholera toxin β chain in DME for 4 min at 37°C. Cells were then washed twice with DME, fixed with 4% PFA for 10 min at RT, and permeabilized with 0.1% Triton X-100 for 10 min at RT. Cells were then analyzed by immunofluorescence for AHNAK and S100A10.

Flotation gradients

For the isolation of lipid rafts, cells grown in 100-mm tissue culture dishes were washed and scraped in PBS, pelleted, and lysed on ice for 30 min in 100 μl Triton X-100 lysis buffer (400 mM Tris, pH 7.5, 150 mM NaCl, 1 mM DTT, 1% Triton X-100, and protease inhibitor cocktail). After a 10-min spin at 2,500 rpm at 4°C, the supernatant was mixed with 200 μl of a 60% OptiPrep™ (Axis-Shield) solution to obtain a 40% final solution, and transferred to centrifuge tubes. The sample was overlayed with 270 μl of a 35, 30, 25, 20, and 5% solution of OptiPrep™ in Triton lysis buffer. The gradient was centrifuged in an ultracentrifuge (Optima TL; Beckman Coulter) at 45,000 rpm for 4 h at 4°C in a rotor (TLS-55; Beckman Coulter). The fractions were collected and analyzed by Western blotting.

Online supplemental material

Fig. S1 shows a Coomassie blue stain of the proteins coimmunoprecipitated with AHNAK. Fig. S2 shows the rearrangement of the actin cytoskeleton in polarized MDCK cells. Fig. S3 shows the specific down-regulation of AHNAK protein by immunofluorescence in MDCK cells treated with AHNAK siRNA. The online supplemental material is available at http://www.jcb.org/cgi/content/full/jcb.200307098/DC1.

We thank Dr. Deloulme for his help with yeast two-hybrid experiments; Dr. D. Grunwald for his help with confocal microscopy (Imaging Core Facility, DRDC, CEA-Grenoble); Dr. Nie and Dr. Hashimoto (Kurume University, Kurume, Japan) for pC-DY plasmid and anti-desmoyokin/AHNAK antibody DY, Dr. Gerke for HH7 antibody, and Dr. Lamarre for critical reading of the manuscript.

This work was supported by grant form the Association pour la Recherche contre le Cancer (ARC 5643 to C. Delphin) and by a fellowship from la Ligue Nationale contre le Cancer (to B.J. Gentil).

Submitted: 15 July 2003
Accepted: 20 November 2003

References

Babiychuk, E.B., and A. Draeger. 2000. Annexins in cell membrane dynamics. Ca^{2+}-regulated association of lipid microdomains. *J. Cell Biol.* 150:1113–1124.

Babiychuk, E.B., K. Monastyrskaya, F.C. Burkhard, S. Wray, and A. Draeger. 2002. Modulating signaling events in smooth muscle: cleavage of annexin 2 abolishes its binding to lipid rafts. *FASEB J.* 16:1177–1184.

Barton, N.R., E.M. Bonder, D.J. Fishkind, R.H. Warren, and M.M. Pratt. 1992. A novel vesicle-associated protein (VAP-1) in sea urchin eggs containing multiple RNA-binding consensus sequences. *J. Cell Sci.* 103:797–809.

Borgonovo, B., E. Cocucci, G. Racchetti, P. Podini, A. Bachi, and J. Meldolesi.

2002. Regulated exocytosis: a novel, widely expressed system. *Nat. Cell Biol.* 4:955–962.

Corvera, S., C. DiBonaventura, and H.S. Shpetner. 2000. Cell confluence-dependent remodeling of endothelial membranes mediated by cholesterol. *J. Biol. Chem.* 275:31414–31421.

Deloulme, J.C., N. Assard, G.O. Mbele, C. Mangin, R. Kuwano, and J. Baudier. 2000. S100A6 and S100A11 are specific targets of the calcium- and zinc-binding S100B protein in vivo. *J. Biol. Chem.* 275:35302–35310.

Deloulme, J.C., B.J. Gentil, and J. Baudier. 2003. Monitoring of S100 homodimerization and heterodimeric interactions by the yeast two-hybrid system. *Microsc. Res. Tech.* 60:560–568.

Downs, K.M., J. McHugh, A.J. Copp, and E. Shtivelman. 2002. Multiple developmental roles of Ahnak are suggested by localization to sites of placentation and neural plate fusion in the mouse conceptus. *Gene Expr. Patterns.* 2:27–34.

Drubin, D.G., and W.J. Nelson. 1996. Origins of cell polarity. *Cell.* 84:335–344.

Dytrych, L., D.L. Sherman, C.S. Gillespie, and P.J. Brophy. 1998. Two PDZ domain proteins encoded by the murine periaxin gene are the result of alternative intron retention and are differentially targeted in Schwann cells. *J. Biol. Chem.* 273:5794–5800.

Gentil, B.J., C. Delphin, G.O. Mbele, J.C. Deloulme, M. Ferro, J. Garin, and J. Baudier. 2001. The giant protein AHNAK is a specific target for the calcium- and zinc-binding S100B protein: potential implications for Ca^{2+} homeostasis regulation by S100B. *J. Biol. Chem.* 276:23253–23261.

Gentil, B.J., C. Delphin, C. Benaud, and J. Baudier. 2003. Expression of the giant protein AHNAK (desmoyokin) in muscle and lining epithelial cells. *J. Histochem. Cytochem.* 51:339–348.

Gerke, V., and K. Weber. 1985. The regulatory chain in the p36-kd substrate complex of viral tyrosine-specific protein kinases is related in sequence to the S-100 protein of glial cells. *EMBO J.* 4:2917–2920.

Gerke, V., and S.E. Moss. 2002. Annexins: from structure to function. *Physiol. Rev.* 82:331–371.

Girard, C., N. Tinel, C. Terrenoire, G. Romey, M. Lazdunski, and M. Borsotto. 2002. p11, an annexin II subunit, an auxiliary protein associated with the background K^+ channel, TASK-1. *EMBO J.* 21:4439–4448.

Grindstaff, K.K., C. Yeaman, N. Anandasabapathy, S.C. Hsu, E. Rodriguez-Boulan, R.H. Scheller, and W.J. Nelson. 1998. Sec6/8 complex is recruited to cell-cell contacts and specifies transport vesicle delivery to the basal-lateral membrane in epithelial cells. *Cell.* 93:731–740.

Haase, H., T. Podzuweit, G. Lutsch, A. Hohaus, S. Kostka, C. Lindschau, M. Kott, R. Kraft, and I. Morano. 1999. Signaling from β-adrenoceptor to L-type calcium channel: identification of a novel cardiac protein kinase A target possessing similarities to AHNAK. *FASEB J.* 13:2161–2172.

Hansen, M.D., J.S. Ehrlich, and W.J. Nelson. 2002. Molecular mechanism for orienting membrane and actin dynamics to nascent cell-cell contacts in epithelial cells. *J. Biol. Chem.* 277:45371–45376.

Harder, T., and V. Gerke. 1993. The subcellular distribution of early endosomes is affected by the annexin II2p11(2) complex. *J. Cell Biol.* 123:1119–1132.

Harder, T., R. Kellner, R.G. Parton, and J. Gruenberg. 1997. Specific release of membrane-bound annexin II and cortical cytoskeletal elements by sequestration of membrane cholesterol. *Mol. Biol. Cell.* 8:533–545.

Harder, T., P. Scheiffele, P. Verkade, and K. Simon. 1998. Lipid domain structure of the plasma membrane revealed by patching of membrane components. *J. Cell Biol.* 141:929–942.

Hashimoto, T., M. Amagai, D.A. Parry, T.W. Dixon, S. Tsukita, K. Miki, K. Sakai, Y. Inokuchi, J. Kudoh, N. Shimizu, and T. Nishikawa. 1993. Desmoyokin, a 680 kDa keratinocyte plasma membrane-associated protein, is homologous to the protein encoded by human gene AHNAK. *J. Cell Sci.* 105: 275–286.

Hashimoto, T., S. Gamou, N. Shimizu, Y. Kitajima, and T. Nishikawa. 1995. Regulation of translocation of the desmoyokin/AHNAK protein to the plasma membrane in keratinocytes by protein kinase C. *Exp. Cell Res.* 217: 258–266.

Hieda, Y., and S. Tsukita. 1989. A new high molecular mass protein showing unique localization in desmosomal plaque. *J. Cell Biol.* 109:1511–1518.

Hohaus, A., V. Person, J. Behlke, J. Schaper, I. Morano, and H. Haase. 2002. The carboxyl-terminal region of ahnak provides a link between cardiac L-type Ca^{2+} channels and the actin-based cytoskeleton. *FASEB J.* 16:1205–1216.

Kingsley, P.D., K.E. McGrath, K.M. Maltby, A.D. Koniski, R. Ramchandran, and J. Palis. 2001. Subtractive hybridization reveals tissue-specific expression of ahnak during embryonic development. *Dev. Growth Differ.* 43:133–143.

Kudoh, J., Y. Wang, S. Minoshima, T. Hashimoto, M. Amagai, T. Nishikawa, E. Shtivelman, J.M. Bishop, and N. Shimizu. 1995. Localization of the human AHNAK/desmoyokin gene (AHNAK) to chromosome band 11q12 by somatic cell hybrid analysis and fluorescence in situ hybridization. *Cytogenet. Cell Genet.* 70:218–220.

McClintock, K.A., L.J. Van Eldik, and G.S. Shaw. 2002. The C-terminus and linker region of S100B exert dual control on protein-protein interactions with TRTK-12. *Biochemistry.* 41:5421–5428.

Nie, Z., W. Ning, M. Amagai, and T. Hashimoto. 2000. C-Terminus of desmoyokin/AHNAK protein is responsible for its translocation between the nucleus and cytoplasm. *J. Invest. Dermatol.* 114:1044–1049.

Oliferenko, S., K. Paiha, T. Harder, V. Gerke, C. Schwarzler, H. Schwarz, H. Beug, U. Gunthert, and L.A. Huber. 1999. Analysis of CD44-containing lipid rafts: Recruitment of annexin II and stabilization by the actin cytoskeleton. *J. Cell Biol.* 146:843–854.

Puisieux, A., J. Ji, and M. Ozturk. 1996. Annexin II up-regulates cellular levels of p11 protein by a post-translational mechanisms. *Biochem. J.* 313:51–55.

Schafer, B.W., and C.W. Heizmann. 1996. The S100 family of EF-hand calcium-binding proteins: functions and pathology. *Trends Biochem. Sci.* 21:134–140.

Sekiya, F., Y.S. Bae, D.Y. Jhon, S.C. Hwang, and S.G. Rhee. 1999. AHNAK, a protein that binds and activates phospholipase C-γ1 in the presence of arachidonic acid. *J. Biol. Chem.* 274:13900–13907.

Shtivelman, E., and J.M. Bishop. 1993. The human gene AHNAK encodes a large phosphoprotein located primarily in the nucleus. *J. Cell Biol.* 120:625–630.

Shtivelman, E., F.E. Cohen, and J.M. Bishop. 1992. A human gene (AHNAK) encoding an unusually large protein with a 1.2-μm polyionic rod structure. *Proc. Natl. Acad. Sci. USA.* 89:5472–5476.

Simons, K., and D. Toomre. 2000. Lipid rafts and signal transduction. *Nat. Rev. Mol. Cell Biol.* 1:31–39.

Sussman, J., D. Stokoe, N. Ossina, and E. Shtivelman. 2001. Protein kinase B phosphorylates AHNAK and regulates its subcellular localization. *J. Cell Biol.* 154:1019–1030.

Van de Graaf, S.F., J.G. Hoenderop, D. Gkika, D. Lamers, J. Prenen, U. Rescher, V. Gerke, O. Staub, B. Nilius, and R.J. Bindels. 2003. Functional expression of the epithelial Ca^{2+} channels (TRPV5 and TRPV6) requires association of the S100A10-annexin 2 complex. *EMBO J.* 22:1478–1487.

Zajchowski, L.D., and S.M. Robbins. 2002. Lipid rafts and little caves. Compartmentalized signalling in membrane microdomains. *Eur. J. Biochem.* 269: 737–752.

Zuber, J., O.I. Tchernitsa, B. Hinzmann, A.C. Schmitz, M. Grips, M. Hellriegel, C. Sers, A. Rosenthal, and R. Schafer. 2000. A genome-wide survey of RAS transformation targets. *Nat. Genet.* 24:144–152.